

## The role of Zn in model nuclear waste glasses studied by XAS

N.J. Cassingham<sup>1</sup>, M.C. Stennett<sup>1</sup>, P.A. Bingham<sup>1</sup>, G. Aquilanti<sup>2</sup> and N.C. Hyatt<sup>1</sup>

<sup>1</sup>Department of Engineering Materials, University of Sheffield

<sup>2</sup>Sincrotrone Trieste, ELETTRA, 34012 Basovizza (TS), Italy

(correspondence: n.c.hyatt@sheffield.ac.uk)

### ABSTRACT

It has been suggested that small additions of zinc increases the durability of oxide glasses of interest for radioactive waste immobilisation. However, the structural environment of Zn in such glasses is not fully understood. To understand the mechanisms by which Zn increases glass durability, a suite of Zn doped model silicate glasses was investigated by Zn K-edge X-ray absorption spectroscopy (XAS) together with a mineral specimen of hemimorphite -  $Zn_4Si_2O_7(OH)_2 \cdot H_2O$  and a simulant UK HLW glass. Fitting of XAS data from the mineral standard permitted reliable determination of four-fold co-ordinate Zn in the model and simulant HLW glasses. XAS data show evidence of intermediate range order, in FT  $\chi(k)$  plots, consistent with Zn-O-Si linkages in all glasses. Thus, Zn is understood to adopt a network intermediate role in model and simulant HLW silicate glasses.

### INTRODUCTION

Several studies have reported improvements in the durability of oxide glasses through small additions of ZnO. <sup>(1-8)</sup> Accordingly, ZnO addition to current UK high level waste (HLW) glass formulations is currently under consideration, both as an aid to processing and product longevity. However, the structural role of Zn in such glasses is the subject of some controversy with evidence for behaviour as a network former or a network modifier. <sup>(9-11)</sup> Previous investigation has determined the presence of either four- or six-fold co-ordinate Zn species in oxide silicate glasses, or a combination of such environments. <sup>(11;12)</sup> Both Zachariasen and Warren's theory of glass structure and Dietzel's crystal field theory classify zinc as a network intermediate, i.e. able to adopt both network former and modifier roles. A study of Zn doped alkali silicate glass compositions suggested Zn acts as a weak network former independent of alkali concentration. <sup>(1)</sup> This study aims to better understand the role of zinc in model soda-lime-silicate and simulant HLW glass systems using X-ray absorption spectroscopy (XAS).

XAS is a useful probe of local structure in materials. It is a particularly useful probe for nuclear waste glasses, which are structurally disordered, allowing the local environment of a given absorber element to be determined. Given the chemical complexity of simulant HLW glasses, which may contain over 20 component oxides, it was considered beneficial to first understand the

structural role of Zn in a suite of model soda-lime silicate (SLS) glasses. Building on this knowledge the Zn environment in (non-radioactive) simulant HLW glasses could be investigated with confidence.

### EXPERIMENTAL PROCEDURE

#### Preparation of glasses

Three sodium calcium zinc silicate (NCZS) glasses were prepared for this study, with 8.0 - 14.5 mol% ZnO. The nominal compositions of these glasses in mol% are given in Table 1. Additionally, an alkali zinc silicate glass was prepared with a stoichiometry equivalent to  $Na_2ZnSi_3O_8$ , which has been previously reported in crystalline form. <sup>(13)</sup> The glasses were batched from sand, limestone, soda ash, and zinc oxide powder to make 300 g of glass after melting.

**Table 1** Compositions of model SLS glasses in mol%

	SiO <sub>2</sub>	Na <sub>2</sub> O	CaO	ZnO
<b>NCZS 3</b>	45.4	23.4	23.2	8
<b>NCZS 3.5</b>	44	22.6	22.4	11
<b>NCZS 4</b>	42.6	21.4	21.5	14.5
<b>NCZS 5</b>	60	20	0	20

The glass batches were melted in a platinum crucible at 1350 °C with 1 hr. batch free after the final charge and stirred with a platinum stirrer for 4 hr. The glasses were cast into a block using a pre-heated steel mould, allowed to cool until the melt would not flow and then placed into an annealing

oven at 450 °C for 1 hr where upon the oven was cooled at 1 °C/min to room temperature.

**XAS Measurements**

Zn K-edge XAS spectra were acquired on beam line BL 11.1 X-ray Absorption Fine Structure (XAFS) at ELETTRA in Basovizza, Italy. The beam line utilized a Si (311) double crystal monochromator, detuned for the purpose of harmonic rejection. The Zn K-edge energy was calibrated by a Zn foil *in situ* during each measurement using a reference ion chamber. Data was acquired in transmission mode at room temperature using finely ground sample dispersed in poly-ethyl-glycol (PEG) to achieve one absorption length and pressed into a 13 mm diameter pellet using a stainless steel uni-axial hydraulic press. The *k*-range scanned during acquisition was typically 3 to 18 Å<sup>-1</sup>.

**XRD Analysis**

Glass samples along with the mineral standard were analyzed using a STOE IP-PSD X-ray diffractometer with Cu K $\alpha$  radiation after XAS measurements. Glass samples were measured in order to insure samples were completely homogeneous and amorphous. The mineral standard was analyzed to verify the mineral standard to be hemimorphite (zinc silicate hydroxide hydrate). Figure 1 plots the XRD pattern of the mineral standard with peaks labelled for hemimorphite and silicon oxide.

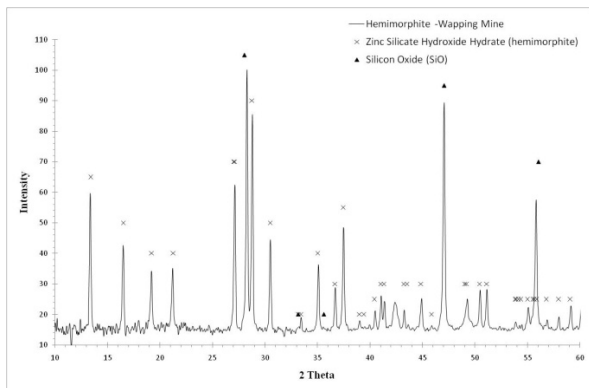


**Figure 1** XRD pattern of the mineral standard used for XAS analysis. Peaks are labelled as either hemimorphite or silicon oxide

**RESULTS AND DISCUSSION**

**XANES analysis**

The X-ray absorption near edge spectroscopy (XANES) data presented in Figure 2 are in good agreement with those reported by McKeown *et al*; however, the superior energy resolution of the (311) monochromator used in this study, ~0.2 eV, permits identification of new features in the near-edge region of the spectra. (5) The SLS glasses and Zn<sub>4</sub>Si<sub>2</sub>O<sub>7</sub>(OH)<sub>2</sub>·H<sub>2</sub>O standard present two spectral features at 9664 and 9668 eV, which are consistent with published theoretical calculations

for tetrahedral Zn species. The XANES spectra are thus all consistent with the presence of ZnO<sub>4</sub> species. (5)

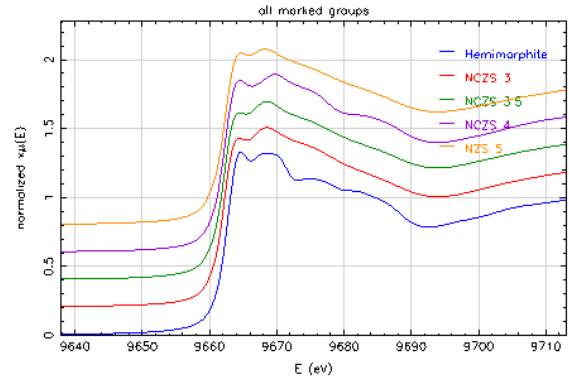


**Figure 2** XAS data for hemimorphite and the four NCZS glasses

**EXAFS analysis**

Extended X-ray absorption fine structure (EXAFS) data were extracted by background subtraction and normalisation of raw spectra. The  $\chi(k)$  data was  $k^3$  weighted and Fourier transformed (FT) over  $3 \leq k \leq 13 \text{ \AA}^{-1}$  with a  $0.5 \text{ \AA}^{-1}$  Hanning window (Figure 3.2). Data analysis was performed with Artemis in the IFEFFIT package. (13)

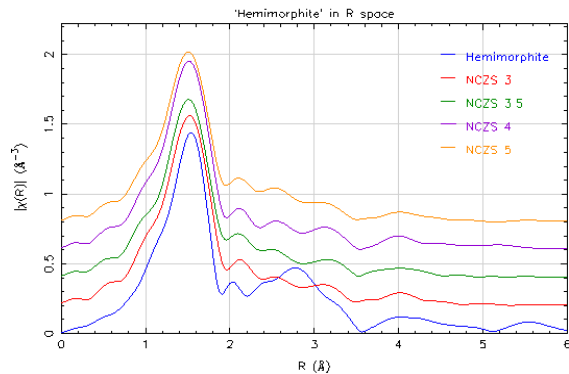


**Figure 3** Fourier transform of  $k^3\chi(k)$  for hemimorphite and the four NCZS glasses

The experimentally determined EXAFS,  $\chi(k)$ , may be considered as the sum of contributions of individual paths associated with the local structure,  $\chi_i(k)$ , as given by the following equations:

$$\chi(k) = \sum_i \chi_i(k) \tag{Eq 1}$$

$$\chi_i(k) \equiv \frac{(N_i S_0^2) F_{eff,i}(k)}{k r_i^2} \sin[2kr_i + \phi_i(k)] e^{-2\sigma_i^2 k^2} \frac{-2r_i}{e^{4(k)}} \tag{Eq 2}$$

Where  $F_{eff}(k)$ ,  $\phi(k)$ , and  $\lambda(k)$  represent, respectively, the effective scattering amplitude, phase shift, and the mean free path of the photoelectron; these are calculated by the IFEFFIT package within Artemis. (13) The distance between the absorber atom and a co-ordinated atom is

denoted by  $r_i$ . The term  $\sigma_i^2$  accounts for the disorder in the interatomic distances and includes contributions from dynamic disorder (thermal vibrations) and static disorder (structural heterogeneity).  $N_i$  represents the number of paths of a given type, corresponding to the co-ordination number for the first shell.  $S_0^2$  is the passive electron reduction factor and accounts for relaxation of remaining electrons in the presence of the core hole which is vacated by the photoelectron in the XAS process. The goodness of fit between the measured and calculated FT  $k^3\chi(k)$  is given by the R-factor.

A key aspect of the current investigation is to determine, accurately, the co-ordination number ( $N_O$ ) of Zn species within the model SLS and simulant HLW glasses. However, as shown in Eq. 2 for the EXAFS formalism  $N_i$  and  $S_0^2$  are completely correlated. Accurate determination of  $N_i$ , therefore, requires independent determination of  $S_0^2$  from a standard material and an assumption of chemical transferability of this parameter between materials (which is generally true for chemically similar species). Therefore,  $S_0^2$  was first determined for Zn in the mineral  $Zn_4Si_2O_7(OH)_2 \cdot H_2O$  (hemimorphite) which is chemically similar to the glasses under study.

**Zn environment in  $Zn_4Si_2O_7(OH)_2 \cdot H_2O$**

In order to verify a four co-ordinate environment around Zn in hemimorphite, according to the published crystal structure, the initial model employed a Zn-O single scattering path with the degeneracy constrained to  $N_O = 4$ . This afforded an adequate fit to the data with  $R = 1.0\%$  and  $S_0^2 = 0.86 \pm 0.03$ . Typically,  $S_0^2$  is determined to lie in the range  $0.8 < S_0^2 < 1.0$ .<sup>(15)</sup> The refined Zn-O contact distance,  $1.95 \pm 0.01 \text{ \AA}$ , and inspection of the FT  $k^3\chi(k)$  data, demonstrated a strong signal at  $1.2 \text{ \AA}$  associated with Zn-O paths and significant intensity near  $2.5 \text{ \AA}$  characteristic of next nearest neighbour scattering paths (distances uncorrected for phase shift, Figure 3). Therefore, additional Zn-Si and Zn-Zn single scattering paths were added with constraints of  $N_{Si} = 3$  and  $N_{Zn} = 4$  in accordance with the published structure.<sup>(16)</sup> Addition of these paths improved the fit with  $R = 0.3\%$  and  $S_0^2 = 0.94 \pm 0.04$ . The final model was in agreement with published crystallographic data, although the refined Zn-Si scattering path was greater by  $\sim 0.5 \text{ \AA}$ , as given in Table 2. However, the refined Zn-Si distance is similar to that determined for the model glasses as reported in the next section.

**Table 2** Comparison between crystallographic data and the final model of  $Zn_4Si_2O_7(OH)_2 \cdot H_2O$

	$N_O$	$N_{Si}$	$N_{Zn}$	$r_{Zn-O}(\text{\AA})$	$\sigma_{Zn-O}^2$	$\pm$	$r_{Zn-Si}(\text{\AA})$	$\sigma_{Zn-Si}^2$	$\pm$	$r_{Zn-Zn}(\text{\AA})$	$\sigma_{Zn-Zn}^2$	$\pm$
$Zn_4Si_2O_7(OH)_2 \cdot H_2O$ Model	4	3	4	1.945	0.005	0.001	3.645	0.004	0.002	3.292	0.010	0.001
Crystallographic Data	4	3	4	1.924	--	--	3.180	--	--	3.333	--	--

**Zn environment in model SLS glasses**

Determination of the Zn co-ordination environment in the model SLS glasses used the same strategy as applied to the  $Zn_4Si_2O_7(OH)_2 \cdot H_2O$  standard. Inspection of FT data revealed features associated with additional next-nearest neighbour scattering paths which were modelled as Zn-Si paths. Refinement of both the Zn co-ordination number ( $N_O$ ) and the number of Zn-Si scattering paths ( $N_{Si}$ ) was stable with  $S_0^2 = 0.94$  as determined from previous analysis. The final models are summarised in Table 3.

**Table 3** Refined models of the four SLS glasses

Sample	$N_O$	$\pm$	$N_{Si}$	$\pm$	R-factor	$r_O(\text{\AA})$	$\pm$	$\sigma_O^2$	$\pm$	$r_{Si}(\text{\AA})$	$\pm$	$\sigma_{Si}^2$	$\pm$
NCZS 3	4.090	0.195	4.228	1.174	0.002	1.947	0.005	0.006	0.001	3.594	0.019	0.016	0.005
NCZS 3.5	3.899	0.197	3.589	1.060	0.002	1.947	0.006	0.006	0.001	3.594	0.014	0.015	0.005
NCZS 4	3.905	0.144	2.247	0.517	0.002	1.943	0.004	0.005	0.001	3.578	0.011	0.008	0.004
NCZS 5	3.794	0.235	3.115	1.037	0.005	1.943	0.007	0.006	0.001	3.596	0.016	0.012	0.006

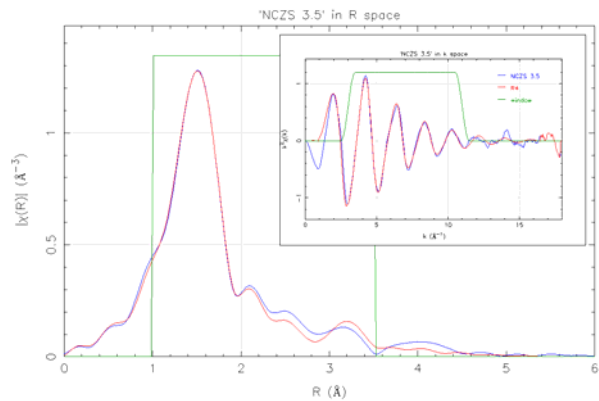


**Figure 4** Example fit of model (red line) to data (blue line) for NCZS 3.5 glass in k- and R-space; green line marks transformation window

The data in Table 3 show that Zn adopts four-fold co-ordination in SLS glasses. Both the refined co-ordination number and refined Zn-O contact distance ( $1.94 \text{ \AA}$ ) are consistent with the formation of tetrahedral  $ZnO_4$  species (e.g.  $1.95 \text{ \AA}$  in  $Zn_4Si_2O_7(OH)_2 \cdot H_2O$ ). This finding is in agreement with previous studies of McKeown *et al* and La Grand *et al*; however, these studies were inconclusive regarding the role of Zn as a network former.<sup>(5; 6)</sup> As shown in Table 3, analysis of EXAFS data is consistent with the presence of Zn-Si contact distances at  $3.59 \text{ \AA}$  similar to that determined for the  $Zn_4Si_2O_7(OH)_2 \cdot H_2O$  standard. The precision associated with the degeneracy of the Zn-Si paths,  $\sim 25\%$ , is reasonable and sufficient to conclusively demonstrate that Zn participates in network formation.

**Zn environment in simulant HLW glass**

The Zn environment in several full scale simulant HLW glasses has also been investigated with similar results to the model SLS glasses. Table 4 gives the refined model for the co-ordination environment of Zn in simulant UK Blend HLW glass (comprising 75% UOX and 25% Magnox fission product waste, the composition is given in Table 5).

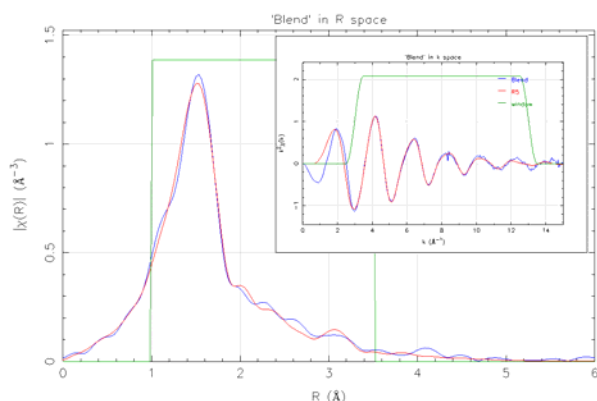
**Table 4** Refined models for the UK Blend HLW simulant waste glass

Model	$N_O$	$\pm$	$N_{Si}$	$\pm$	R-factor	$S_0^2$	$r_O$ (Å)	$\pm$	$\sigma_O^2$	$\pm$	$r_{Si}$ (Å)	$\pm$	$\sigma_{Si}^2$	$\pm$
Zn-O	4.21	0.20	--	--	0.001	0.86	1.95	0.01	0.01	0.00	--	--	--	--
Zn-O-Si	4.17	0.25	2.54	1.03	0.004	0.94	1.94	0.01	0.01	0.00	3.59	0.02	0.01	0.01

**Table 5** Nominal composition of the simulant UK Blend HLW waste glass

Oxide	Mol %	Oxide	Mol %
Al <sub>2</sub> O <sub>3</sub>	1.01	RuO <sub>2</sub>	0.00
BaO	0.15	Sm <sub>2</sub> O <sub>3</sub>	0.08
CeO <sub>2</sub>	0.45	SrO	0.18
Cr <sub>2</sub> O <sub>3</sub>	0.19	TeO <sub>2</sub>	0.09
Cs <sub>2</sub> O	0.33	Y <sub>2</sub> O <sub>3</sub>	0.07
Fe <sub>2</sub> O <sub>3</sub>	0.72	ZrO <sub>2</sub>	1.10
Gd <sub>2</sub> O <sub>3</sub>	0.63	SiO <sub>2</sub>	52.12
La <sub>2</sub> O <sub>3</sub>	0.12	B <sub>2</sub> O <sub>3</sub>	18.24
MgO	2.08	Na <sub>2</sub> O	10.28
MoO <sub>3</sub>	0.85	CaO	1.76
Nd <sub>2</sub> O <sub>3</sub>	0.35	ZnO	3.85
NiO	0.25	Li <sub>2</sub> O	5.00
Pr <sub>2</sub> O <sub>3</sub>	0.11		

The same strategy was employed to fit the EXAFS data from simulant UK HLW glasses, as for the model SLS compositions assuming  $S_0^2 = 0.94$ . The FT  $k^3\chi(k)$  data, provided evidence for intermediate range order as shown by the intensity near 2.5 Å in Figure 5. This feature could be fitted by assuming Zn-Si next nearest neighbour scattering as shown in Table 4.


**Figure 5** Illustrating example fit of model (red line) to data (blue line) for blend HLW glass in k- and R-space; green line marks transformation window

The refined Zn co-ordination number and Zn-O path length of 1.94 Å are again consistent with the presence of tetrahedral ZnO<sub>4</sub> species. The precision associated with the degeneracy of the Zn-Si paths, ~50%, is large and does not allow conclusive determination of the presence of intermediate range order associated with next nearest neighbours. However, the refined Zn-Si distance and corresponding features in the FT  $k^3\chi(k)$  data are consistent with the presence of co-ordinated silicate species by comparison with data from simple SLS compositions.

## CONCLUSIONS

An XAS investigation of model SLS and simulant HLW glasses has demonstrated the presence of

tetrahedral ZnO<sub>4</sub> species. Importantly, this study has also demonstrated, conclusively, that Zn engages in network formation in SLS and HLW glass compositions adopting a network intermediate role as expected from current theoretical models of glass structure. Further work to understand Zn speciation in hydrothermally altered and radiation damaged glasses is underway.

## REFERENCES

- Lusvardi, G., Malavasi, G., Menabue, L., Menziani, M.C. 2002, *J. of Phys. and Chem. B*, Vol. 106, pp. 9753-9760.
- Lusvardi, G., Malavasi, G., Menabue, L., Menziani, M.C., Segre, U., Carnasciali, M.M., Ubaldini, A. 2004, *J. of Non-Cryst. Sol.*, Vol. 345 & 346, pp. 710-714.
- Musinu, A., Piccaluga, G. and Magini, M. 5, 1988, *J. of the Amer. Ceram. Soc.*, Vol. 71, pp. C-256 -- C-259.
- Ennas, G., Musinu, A., Piccaluga, G., Montenero, A., Gnappi, G. 1990, *J. of Non-Cryst. Sol.*, Vol. 125, p. 181.
- McKeown, D.A., Muller, I.S., Buechele, A.C., Pegg, I.L. 2000, *J. of Non-Cryst. Sol.*, Vol. 261, pp. 155-162.
- Le Grand, M., Ramos, A.Y., Calas, G., Galois, L., Ghaleb, D., Pacaud, F. 9, 2000, *J. of Mat. Res. Soc.*, Vol. 15, pp. 2015-2019.
- Della MEA, G., Gasparotto, A., Bettinelli, M., Montenero, A., Scaglioni, R. 1986, *J. of Non-Cryst. Sol.*, Vol. 84, p. 443.
- Minser, D. G., Walden, B. and White, W. B. 1984, *Comm. of the Amer. Ceram. Soc.*, pp. C-47.
- Rosenthal, A. B. and Garofalini, S. H. 1986, *J. of Non-Cryst. Sol.*, Vol. 87, pp. 254-262.
- Rosenthal, A. B. and Garofalini, S. H. 92, 1987, *J. of Non-Cryst. Sol.*, pp. 354-362.
- Hurt, J. C. and Phillips, C. J. 5, 1970, *J. of the Amer. Ceram. Soc.*, Vol. 53, pp. 269-273.
- Rosenthal, A. B. and Garofalini, S. H. 11, 1987, *J. of the Amer. Ceram. Soc.*, Vol. 70, pp. 821-826.
- Ravel, B. and Newville, M. 2005, *J. of Synch. Rad.*, Vol. 12, pp. 537-541.
- Dumas, T. and Petiau, J. 1986, *J. of Non-Cryst. Sol.*, Vol. 81, pp. 201-220.
- Hesse, K. F., et al. 5, May 1977, *Acta Crysta B*, Vol. 33, pp. 1333-1337.
- Ito, T. and West, J. 1932, *Zeitschrift fuer Kristallographie*, Vol. 83, pp. 1-8.

## ACKNOWLEDGEMENT

The research leading to these results has received funding from the European Community's Seventh Framework Programme (FP7/2007-2013) under grant agreement n° 226716. The authors are grateful for allocation of beam time at the ELETTRA light source.